RESEARCH ARTICLE

Figures and figure supplements

Stabilisation of HIF signalling in the mouse epicardium extends embryonic potential and neonatal heart regeneration

Elisabetta Gamen *et al*.

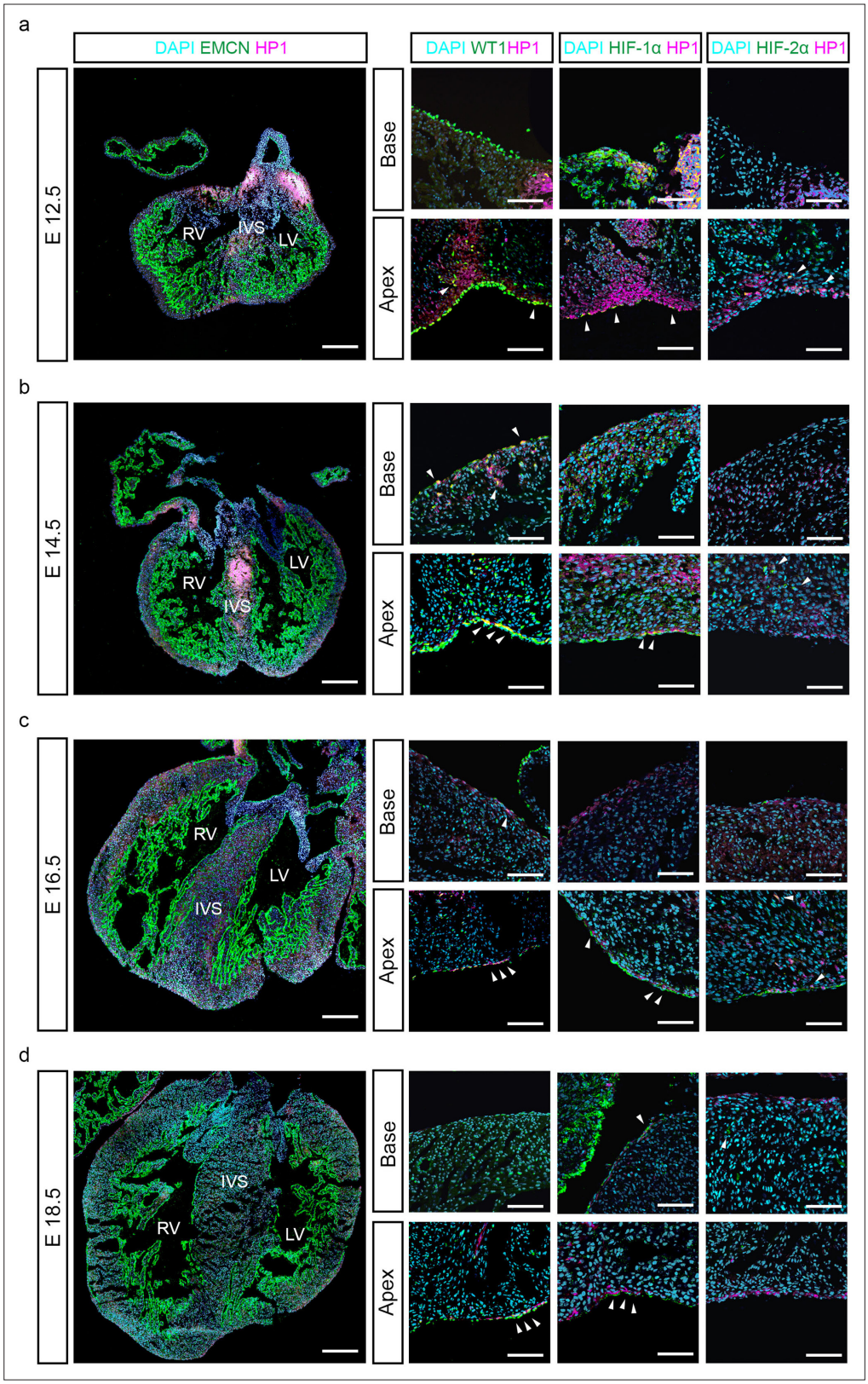

Figure 1. The epicardium is hypoxic at later stages of heart development. Representative images of immunostaining for DAPI (cyan), HP1 (magenta) and EMCN, WT1, HIF-1α and HIF-2α (green) on serial cryosections of foetal hearts at E12.5 (**a**), E14.5 (**b**), E16.5 (**c**), and E18.5 (**d**). Arrowheads indicate overlap between HP1 and WT1, HIF-1α or HIF-2α. n=6 hearts per stage. IVS = interventricular septum, RV = right ventricle, LV = left ventricle. Whole heart scale bars, 200 μm; high-magnification scale bars, 100 μm.

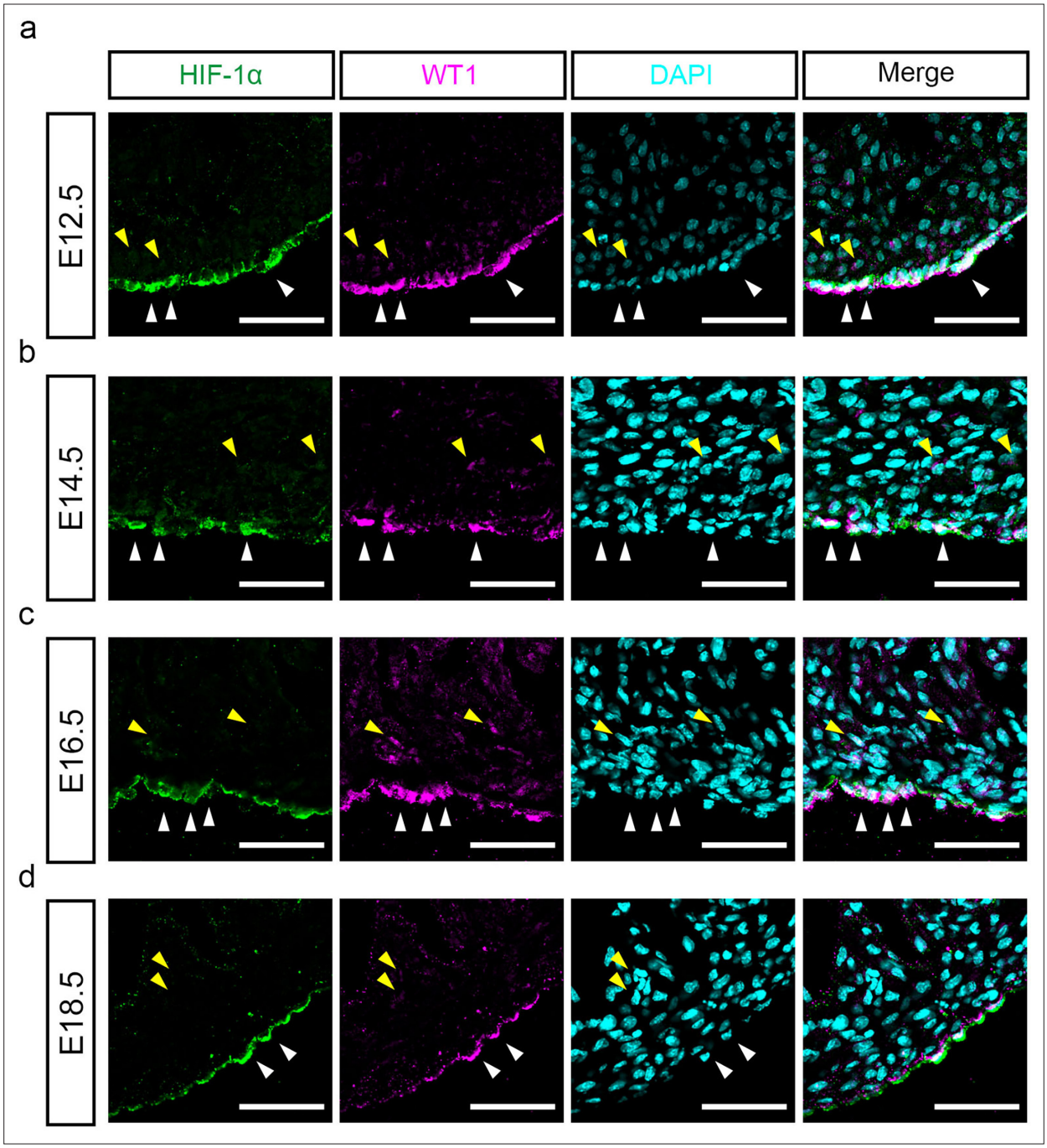

Figure 1—figure supplement 1. HIF-1α is expressed in the epicardium at different stages of heart development. Representative images of immunostaining for DAPI (cyan), HIF-1α (green), and WT1 (magenta) on apical regions of foetal hearts at E12.5 (**a**), E14.5 (**b**), E16.5 (**c**), and E18.5 (**d**). White arrowheads indicate HIF-1α expression in epicardial WT1-expressing cells. Yellow arrowheads indicate WT1-expressing cells lacking HIF-1α expression in the myocardial compartment. n=3 hearts per stage. Scale bar, 50 μm.

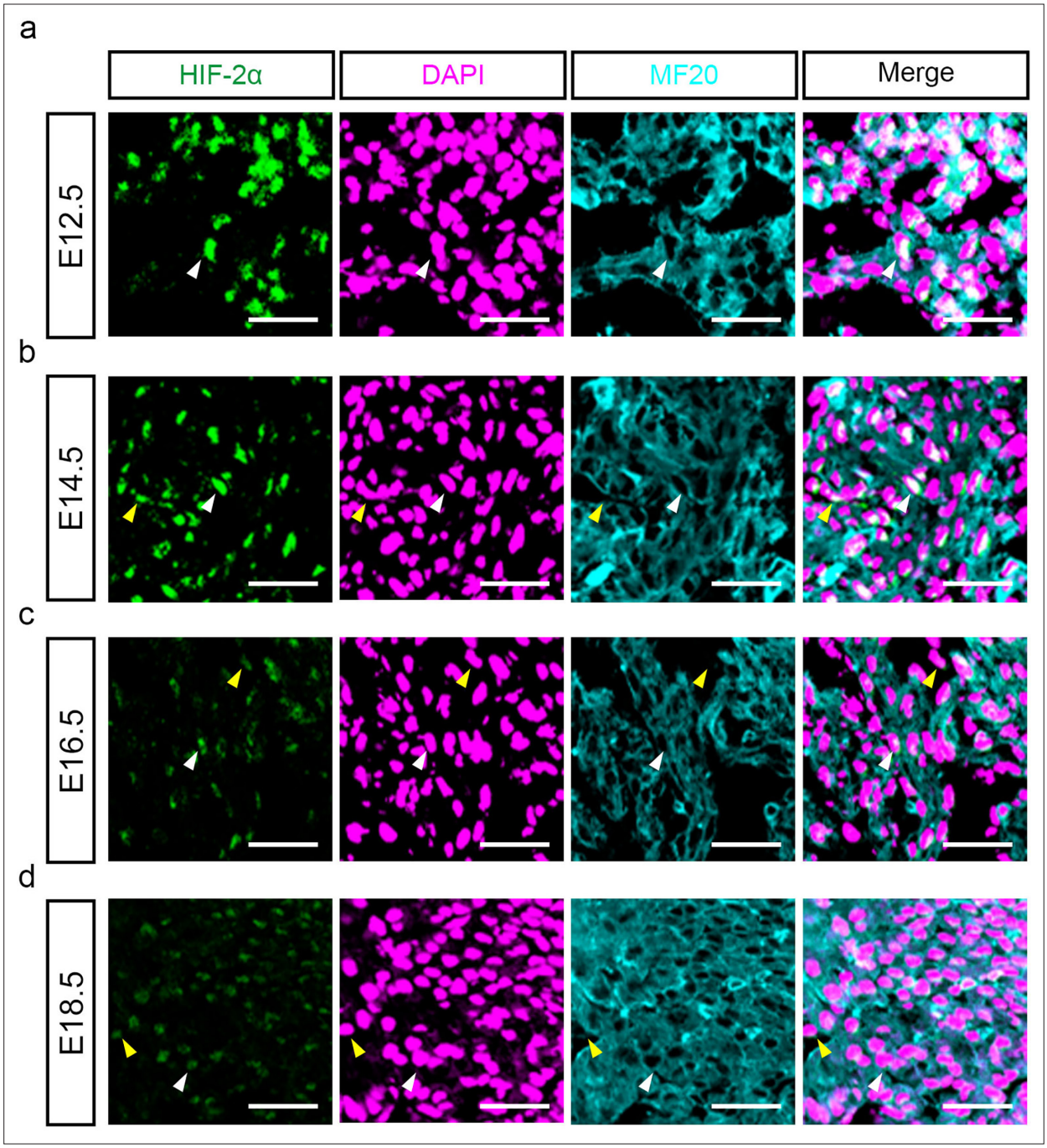

Figure 1—figure supplement 2. HIF-2α is expressed in the myocardium at different stages of heart development. Representative images of immunostaining for DAPI (magenta), HIF-2α (green), and MF20 (cyan) on cryosections of foetal hearts at E12.5 (**a**), E14.5 (**b**), E16.5 (**c**), and E18.5 (**d**). White arrowheads indicate HIF-2α expression in cardiomyocytes. Yellow arrowheads indicate HIF-2α expression in non-cardiomyocyte cells. n=3 hearts per stage. Scale bar, 50 μm.

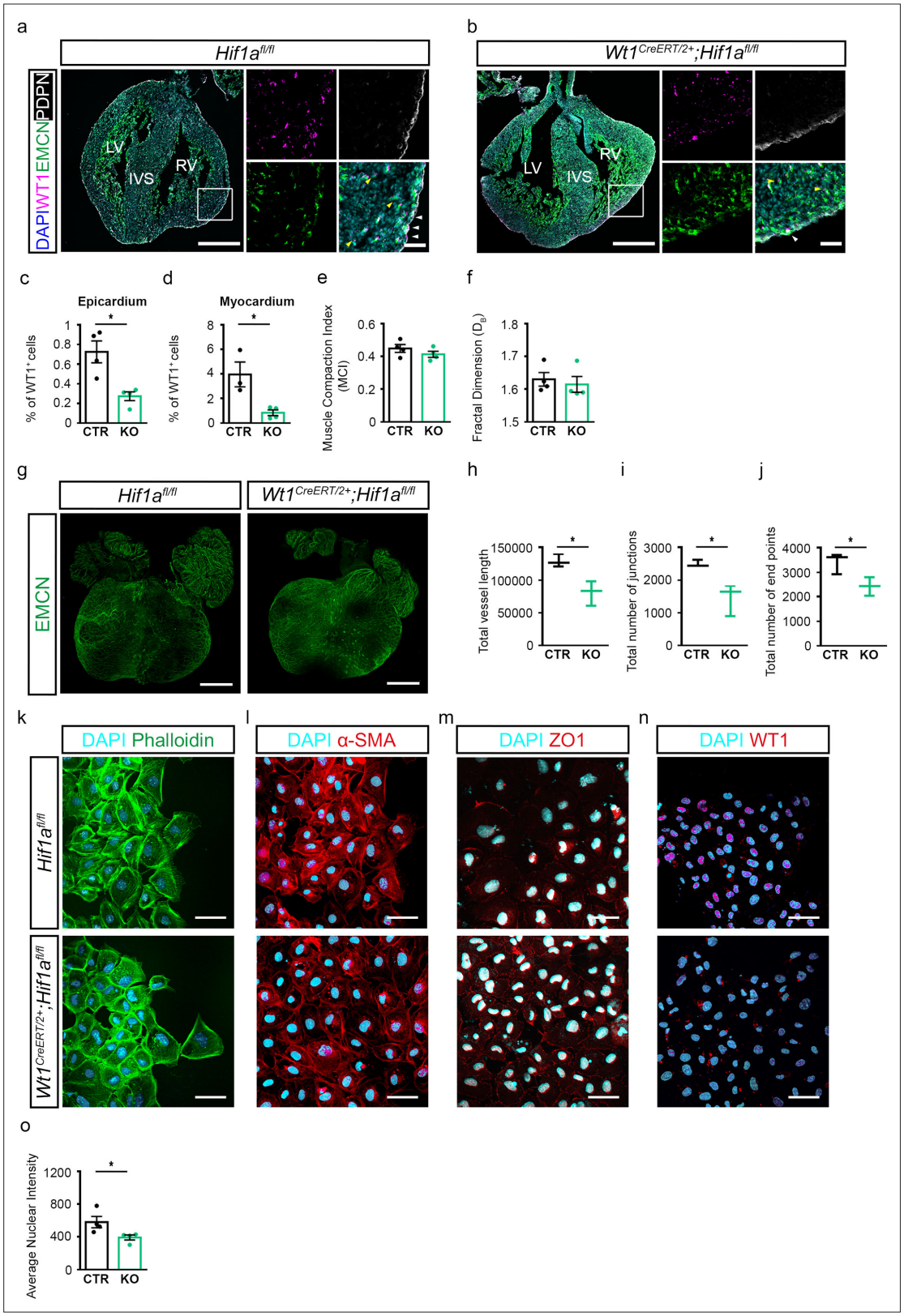

Figure 2. Epicardial loss of *Hif1a* leads to reduced WT1 expression and impaired EMT. (**a, b**) Representative images of immunostaining for EMCN (green), WT1 (magenta), PDPN (white), and DAPI (blue), on coronal sections of hearts from (**a**) *Hif1a*$^{fl/fl}$ (CTR) or (**b**) *Wt1*$^{CreERT2/+}$;*Hif1a*$^{fl/fl}$ (KO) embryos injected with tamoxifen at E9.5 and E10.5 and harvested at E16.5. Images on the right of each panel represent high magnifications of boxed regions. White arrowheads indicate WT1-expressing cells in the epicardium. Yellow arrowheads indicate WT1-expressing cells in the myocardial compartment.

Figure 2 continued on next page

Figure 2 continued

Quantification of WT1+ cells in (**c**) the epicardium (CTR, n=4; KO, n=4) or (**d**) the myocardium (CTR, n=4; KO, n=4). (**e**) Muscle compaction index and (**f**) fractal dimension analysis to assess the complexity of myocardial trabeculae. (CTR, n=4; KO, n=4). (**g**) Whole-mount immunostaining for EMCN (green) to visualise the coronary vasculature of CTR and KO embryos at E16. 5. (**h–j**) Quantification of coronary vasculature as (**h**) total vessel length, (**i**) number of junctions, and (**j**) end points carried out using AngioTool. n=3 hearts/group. Representative images of immunostaining for (**k**) Phalloidin (green), (**l**) α smooth muscle actin (α-SMA, red), (**m**) zonula occludens-1 (ZO-1, red), (**n**) WT1 (red) and DAPI nuclear stain (cyan) on epicardial explants derived from *Hif1a*$^{fl/fl}$ (CTR) and *Wt1*$^{CreERT2/+}$;*Hif1a*$^{fl/fl}$(KO) hearts harvested at E11.5. (**o**) Quantification of nuclear intensity of WT1 signal on epicardial explants (CTR, n=4; KO, n=4). IVS = interventricular septum, LV = left ventricle, RV = right ventricle. Whole heart scale bars, 500 μm; high-magnification scale bars, 50 μm. Data presented as median, inter-quartile range (IQR) and upper and lower limits. Error bars represent mean ± s.e.m. *n* numbers refer to individual mice. Two-tailed, unpaired Student t-tests were used for statistical analysis. *p<0.05.

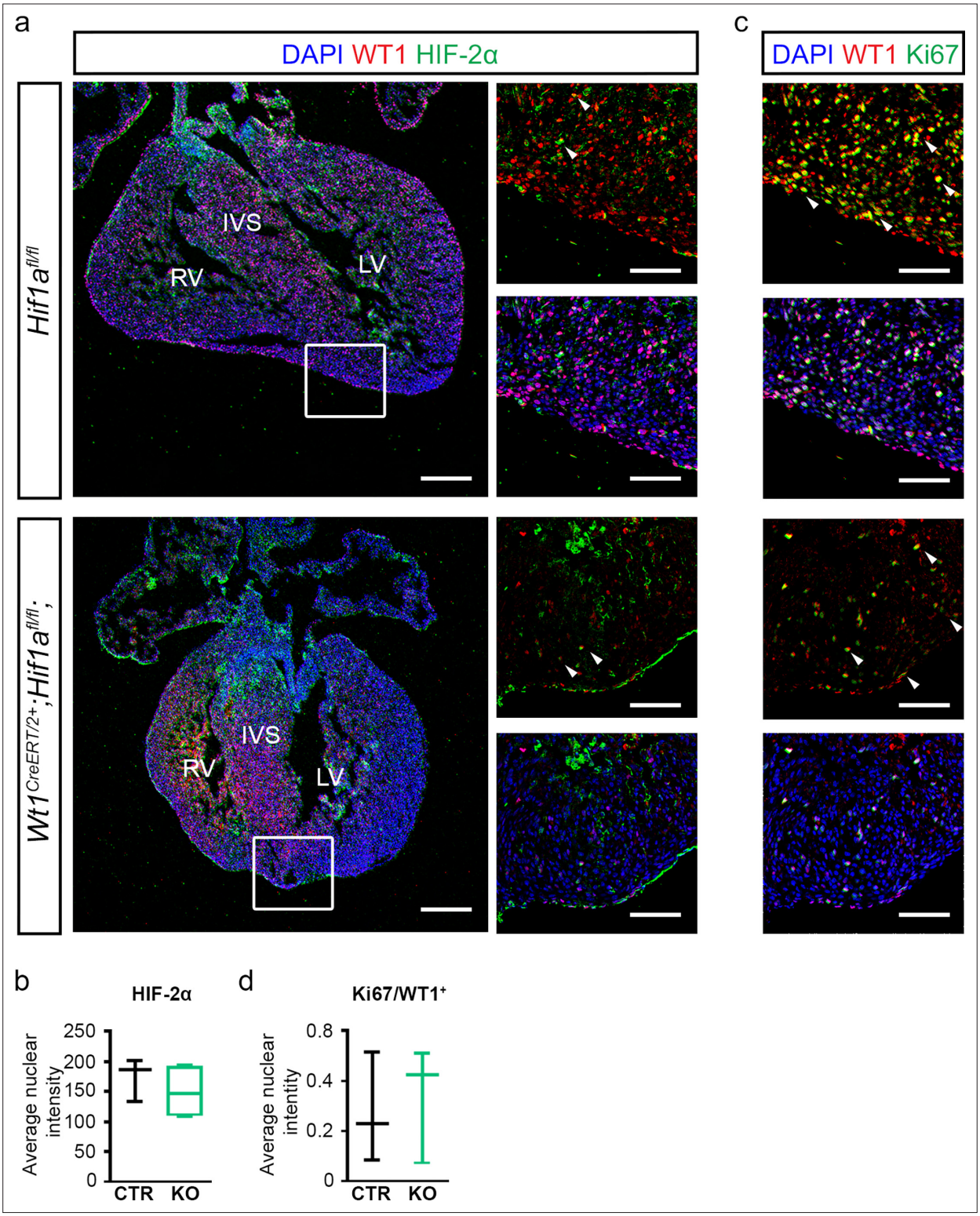

Figure 2—figure supplement 1. Epicardial deletion of HIF-1α does not alter HIF-2α expression nor proliferation of WT1⁺ cells. (**a**) Representative images of co-immunostaining for WT1 (red) and HIF-2α (green) and DAPI nuclear stain (blue) and (**b**) quantification of HIF-2α nuclear signal in WT1+ cells on sections from *Hif1a*$^{fl/fl}$ (CTR, n=3) and *Wt1*$^{CreERT2/+}$;*Hif1a*$^{fl/fl}$ (KO, n=4) hearts harvested at E16.5. (**c**) Representative images of co-immunostaining for WT1 (red), Ki67 (green) and DAPI nuclear stain (blue) and (**d**) quantification of Ki67 nuclear signal in WT1+ cells on section from CTR (n=3) and KO (n=3) hearts harvested at E16.5. Whole heart scale bars, 200 μm; high-magnification scale bars, 100 μm. IVS = interventricular septum, LV = left ventricle, RV = right ventricle. Arrowheads indicate co-expression of WT1 and (**a**) HIF-2α or (**b**) Ki67. Data presented as median, IQR and upper and lower limits. *n* numbers refer to individual mice. Two-tailed, unpaired Student t-tests were used for statistical analysis.

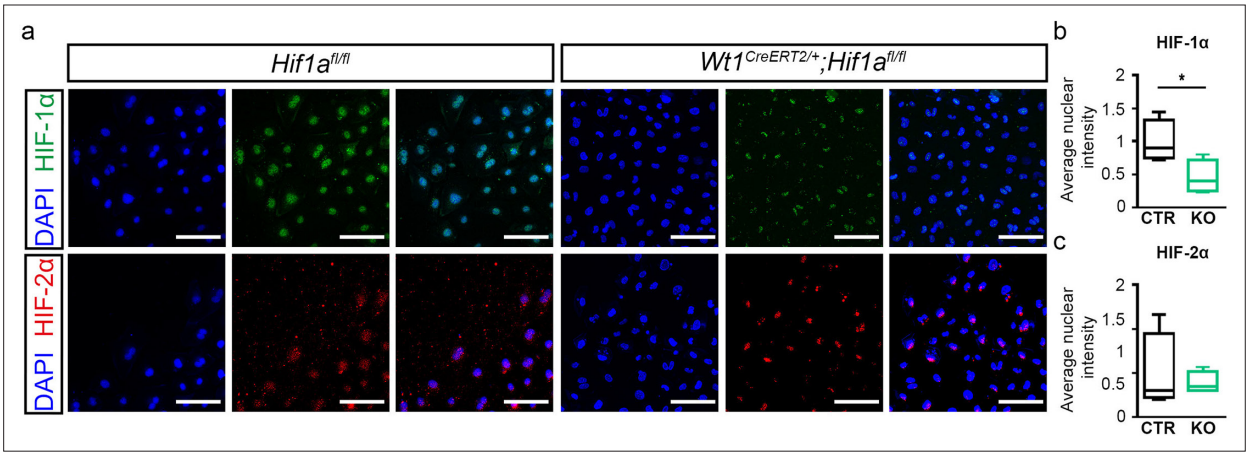

Figure 2—figure supplement 2. Tamoxifen treatment of *Wt1*$^{CreERT2/+}$;*Hif1a*$^{fl/fl}$ -derived epicardial explants reduces HIF-1α expression without affecting HIF-2α. (**a**) Representative images of co-immunostaining for HIF-1α (green), HIF-2α (red), and DAPI nuclear stain (blue) and quantification of (**b**) HIF-1α and (**c**) HIF-2α nuclear signal from E11.5 derived epicardial explants of *Hif1a*$^{fl/fl}$ (CTR, n=4) and *Wt1*$^{CreERT2/+;}$*Hif1a*$^{fl/fl}$ (KO, n=4). Scale bars, 100 μm. Data presented as median, IQR, and upper and lower limits. *n* numbers refer to individual mice. Two-tailed, unpaired Student t-tests were used for statistical analysis. *p<0.05.

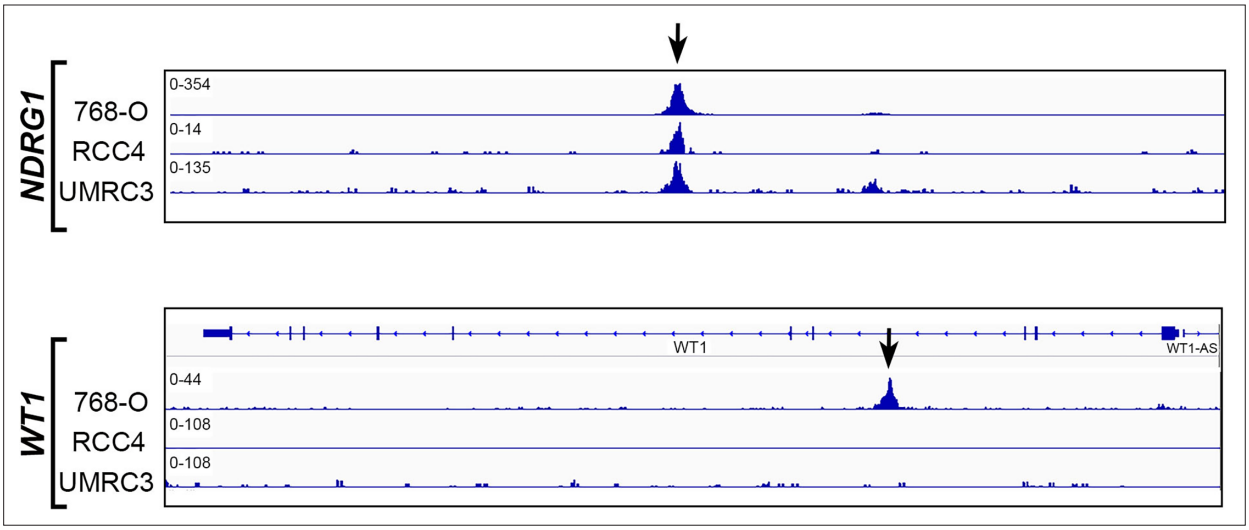

Figure 2—figure supplement 3. HIF-1β subunit directly binds to the WT*1* locus. HIF1β ChIP-sequencing analysis of *NDRG1* (positive control) and *WT1* loci, conducted on human clear cell renal cell carcinoma (ccRCC) line 786-O. Arrows highlight positive peaks.

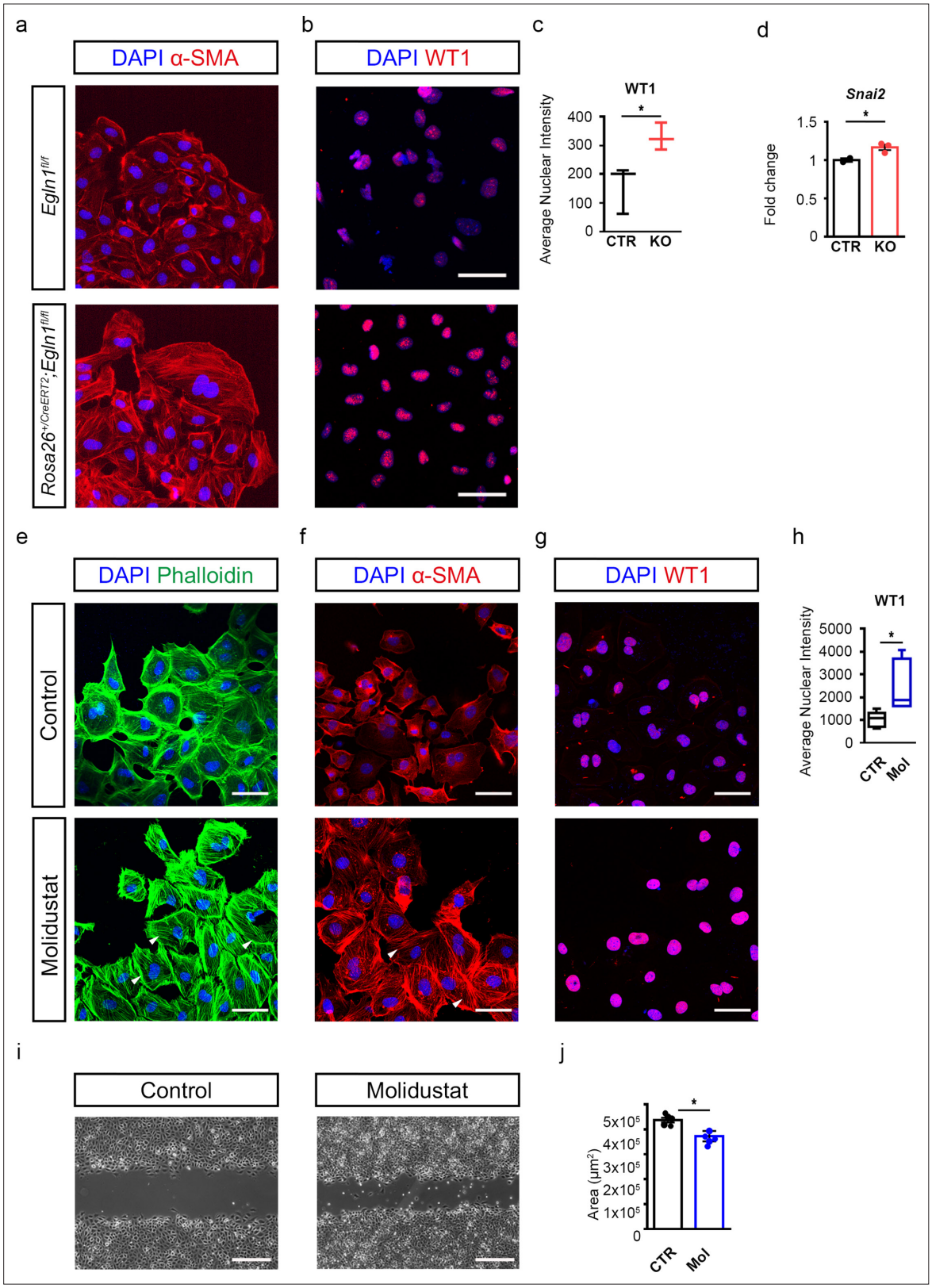

Figure 3. Stabilisation of HIF signalling promotes Wt1 expression and enhances epicardial EMT. (**a, b**) Representative images of immunostaining for α smooth muscle actin (α-SMA, red), WT1 (red), and DAPI nuclear stain (blue) and (**c**) quantification of nuclear intensity of WT1 signal on epicardial explants derived from *Egln1*$^{fl/fl}$ (CTR) and *Rosa26*$^{+/CreERT2}$; *Egln1*$^{fl/fl}$ (KO) embryos at E11.5. n=5 hearts/group. (**d**) *Snai2* expression analysis by qRT-PCR using RNA isolated from epicardial explants derived from CTR (n=2) and KO (n=3) hearts. (**e–g**) Representative images of immunostaining for Phalloidin

Figure 3 continued on next page

Figure 3 continued

(green), α-SMA (red), WT1 (red) and DAPI nuclear stain (blue), and (**h**) quantification of nuclear intensity of WT1 signal on epicardial explants derived from wild type hearts harvested at E11.5 and treated with DMSO (control, CTR, n=6) or Molidustat (Mol, n=6). Scale bars, 50 μm. Arrowheads indicate stress fibres. *n* numbers refer to individual mice. (**i**) Representative images and (**j**) quantification of cell migration assessed by wound healing/scratch assay of MEC.1 cells treated with DMSO (control, CTR, n=5), or Molidustat (Mol, n=5). *n* numbers refer to technical replicates. Scale bars, 0.5 μm. Data presented as median, inter-quartile range (IQR) and upper and lower limits or mean ± *s.e.m.* Two-tailed, unpaired Student t-tests were used for statistical analysis. *p<0.05.

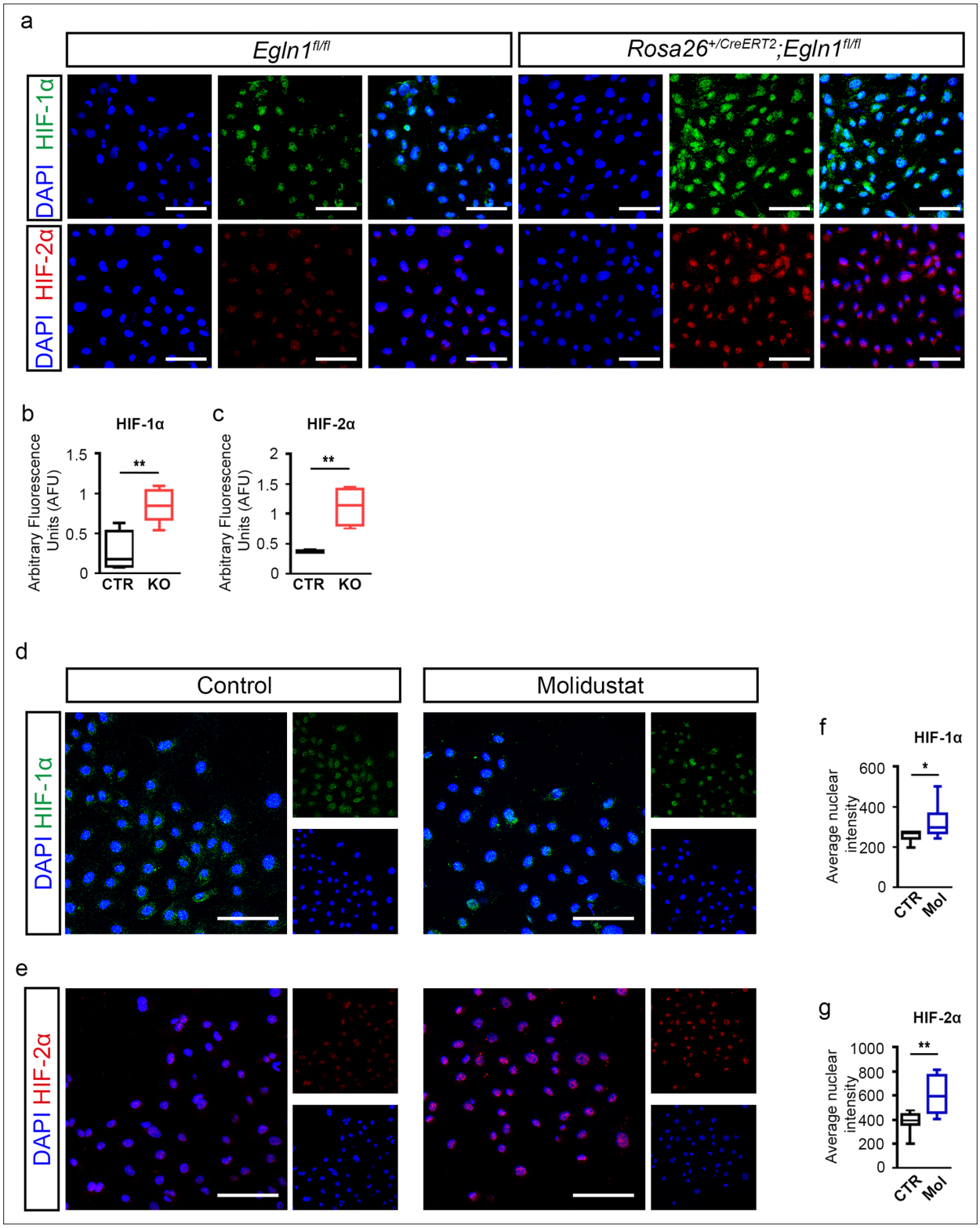

Figure 3—figure supplement 1. Genetic and pharmacological stabilisation of HIF signalling induces both HIF-1α and HIF-2α expression in epicardial explants. (**a**) Representative images of co-immunostaining for HIF-1α (green), HIF-2α (red), and DAPI nuclear stain (blue) on epicardial explants derived from E11.5 hearts of *Egln1*$^{fl/fl}$ (CTR) and *Rosa26*$^{+/CreERT2}$; *Egln1*$^{fl/fl}$ (KO) embryos. Quantification of (**c**) HIF-1α and (**d**) HIF-2α nuclear signal. N=4/group. (**d, e**) Representative images of co-immunostaining for HIF-1α (green), HIF-2α (red) and DAPI nuclear stain (blue) on epicardial explants derived from E11.5 hearts of wild type embryos treated with DMSO (Control), or Molidustat (BAY 85–3934). Quantification of (**f**) HIF-1α and (**g**) HIF-2α nuclear signal from control (CTR, n=4) and Molidustat (Mol, n=4). Scale bars, 100 μm. Data presented as median, IQR and upper and lower limits. *n* numbers refer to individual mice. Two-tailed, unpaired Student t-tests were used for statistical analysis. *p<0.05, **p<0.01.

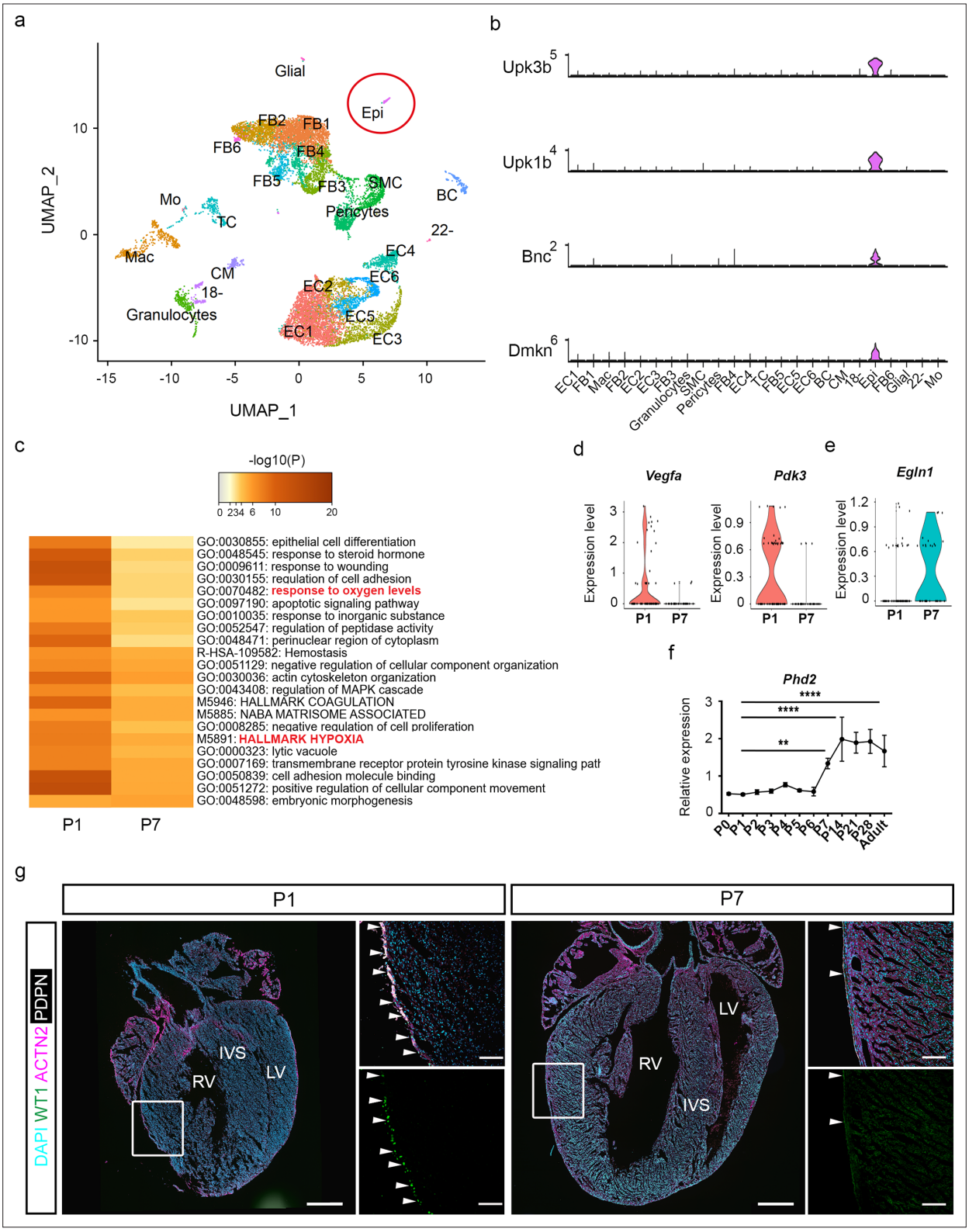

Figure 4. HIF signalling is downregulated in between P1 and P7 in neonatal mice. (**a**) UMAP representation of different cell populations in the intact neonatal heart at postnatal day (P) 1 and P7. (**b**) Stacked violin plots showing expression of canonical Epi-enriched genes *Upk3b*, *Upk1b*, *Bnc*, *Dmkn*. (**c**) Heatmap showing biological processes enriched in the Epi cluster at P1 versus P7. Violin plots showing expression of HIF target genes (**d**) *Vegfa* and *Pdk3*, and (**e**) *Egln1* at P1 versus P7. (**f**) Real time RT-PCR analysis of *Egln1*, n=4 hearts per group. (**g**) Representative images of immunostaining for WT1 (green), ACTN2 (magenta), PDPN (white), and DAPI nuclear stain (cyan) at P1 and P7. Images to the right are magnified views of boxed regions shown

Figure 4 continued on next page

Figure 4 continued

in whole heart images. Arrowheads indicate expression of WT1 in the epicardium. IVS = interventricular septum, LV = left ventricle, RV = right ventricle. Whole heart scale bars, 200 μm; high-magnification scale bars, 100 μm. n=4 hearts per stage. Data are presented as mean ± s.e.m. *n* numbers refer to individual mice. One-way ANOVA with Tukey's post-hoc tests was used for statistical analysis. **p<0.01; ****p<0.0001. Epi, epicardium.

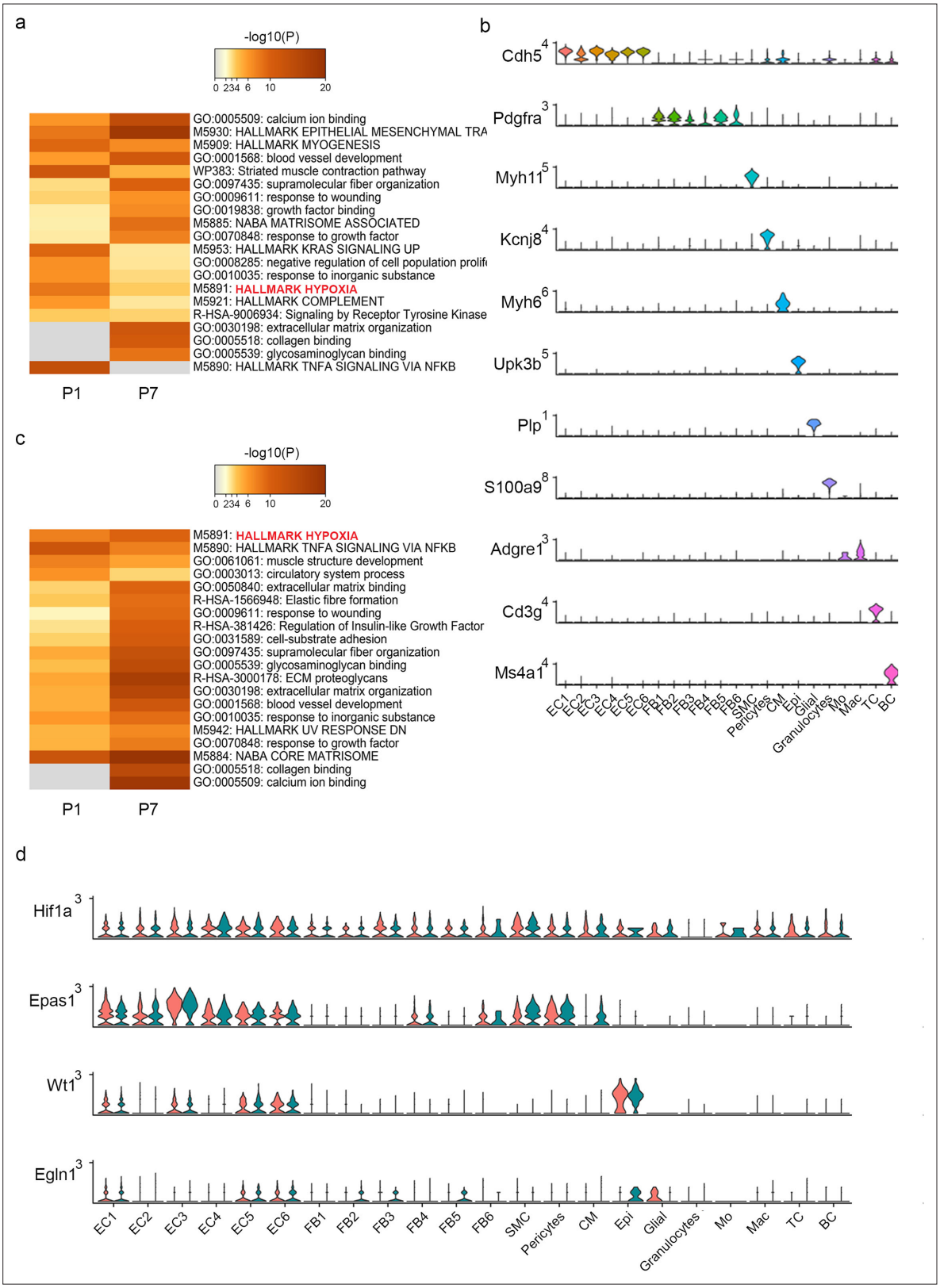

Figure 4—figure supplement 1. Differential activity of HIF signalling in the neonatal mouse. (**a**) Heatmap showing biological processes enriched in all cell populations from intact P1 and P7 hearts. (**b**) Stacked violin plots showing expression of canonical enriched genes for each cell cluster. (**c**) Heatmap showing biological processes enriched in the fibroblast cluster at P1 and P7. (**d**) Stacked violin plots showing expression of *Hif1a*, *Epas1* or *Hif2a*, *Wt1*, and *Egln1* genes for each cell cluster. Red violin represents P1-derived cells, green violin represents P7-derived cells. EC, endothelial cells; FB, fibroblast; SMC, smooth muscle cells; CM, cardiomyocyte; Epi, epicardium; Mo, monocytes; Mac, macrophages; TC, T-cells; BC, B-cells.

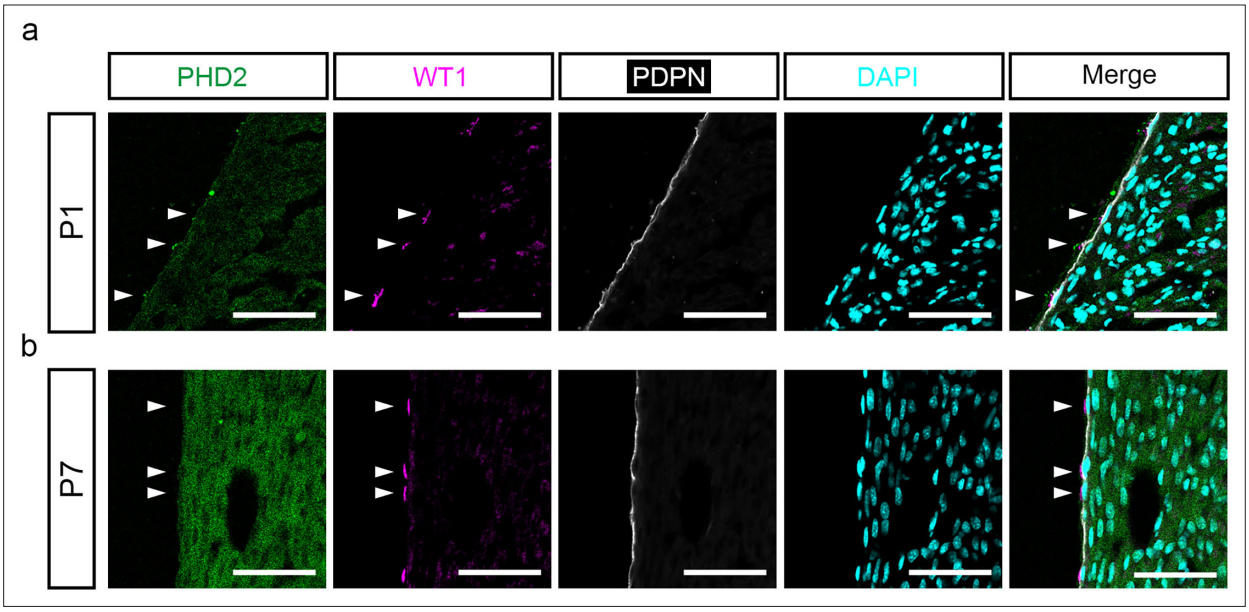

Figure 4—figure supplement 2. PHD2 expression increases in the neonatal heart from P1 to P7. Representative images of immunostaining for PHD2 (green), WT1 (magenta), PDPN (grey), and DAPI (cyan) on cryosections of postnatal (right) ventricles of P1 (**a**) and P7 hearts (**b**). Arrowheads indicate PHD2 expression in $WT1^{+}$ cells. n=3 hearts per stage. Scale bar, 50 μm.

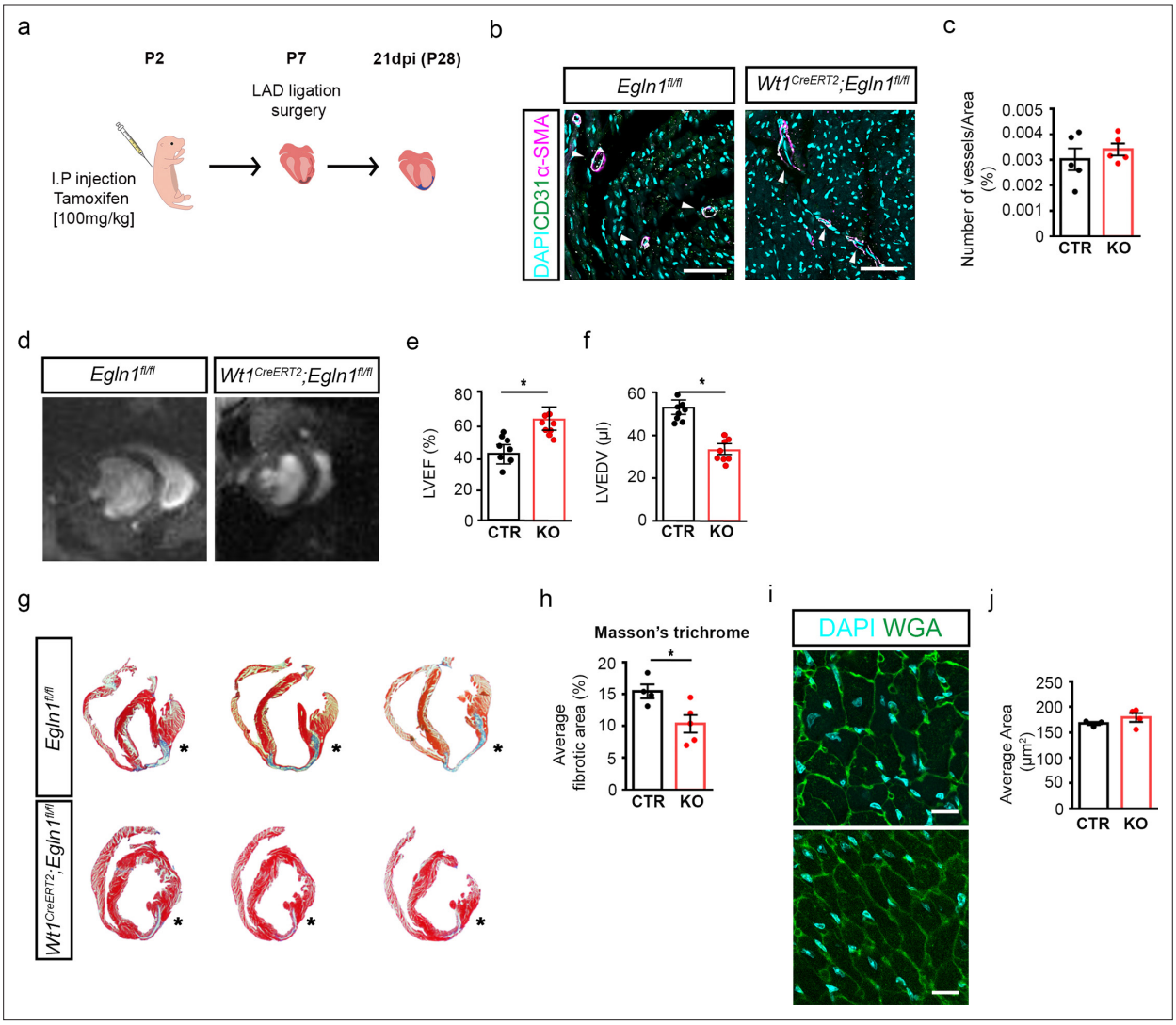

Figure 5. Loss of *Egln1* (PHD2) in WT1 expressing cells improves heart regeneration post-MI. (**a**) Schematic of experimental design. (**b**) Representative images of immunostaining for α-smooth muscle actin (α-SMA, magenta), CD31 (green), and DAPI nuclear stain (cyan) on sections of hearts from *Egln1*$^{fl/fl}$ (CTR, n=5) and *Wt1*^{CreERT2}; *Egln1*$^{fl/fl}$ (KO, n=5) mice and (**c**) quantification of number of vessels at 21 days post-injury (dpi). Arrowheads indicate vessels (determined by co-expression of CD31 and α-SMA). Scale bars, 100 µm. (**d**) Representative mid-ventricular short-axis MRI frames for *Egln1*$^{fl/fl}$ (CTR) and *Wt1*^{CreERT2}; *Egln1*$^{fl/fl}$ (KO) mice hearts. (**e, f**) MRI analyses of infarcted hearts at 21 dpi showing increased EF (**e**) and reduced EDV (**f**) in *Wt1*^{CreERT2}; *Egln1*$^{fl/fl}$ (KO, n=8) animals compared with controls (CTR, n=8). (**g**) Representative images and (**h**) quantification of Masson's Trichrome stained transverse serial sections to assess cardiac fibrosis (blue) at 21 dpi. * denotes suture placement. (**i**) Representative images of immunostaining for wheat-germ agglutinin (WGA, green) and DAPI nuclear stain (cyan) on hearts from control and Molidustat treated mice 21dpi for: Scale bars, 100µm. (**g**) Quantification of cardiomyocyte cell size, as assessed by WGA staining on sections of hearts from CTR (n=4) and KO (n=4). Left ventricular regions were measured. Error bars represent mean ± *s.e.m. n* numbers refer to individual mice. Two-tailed, unpaired Student t-tests were used for statistical analysis. *p<0.05.

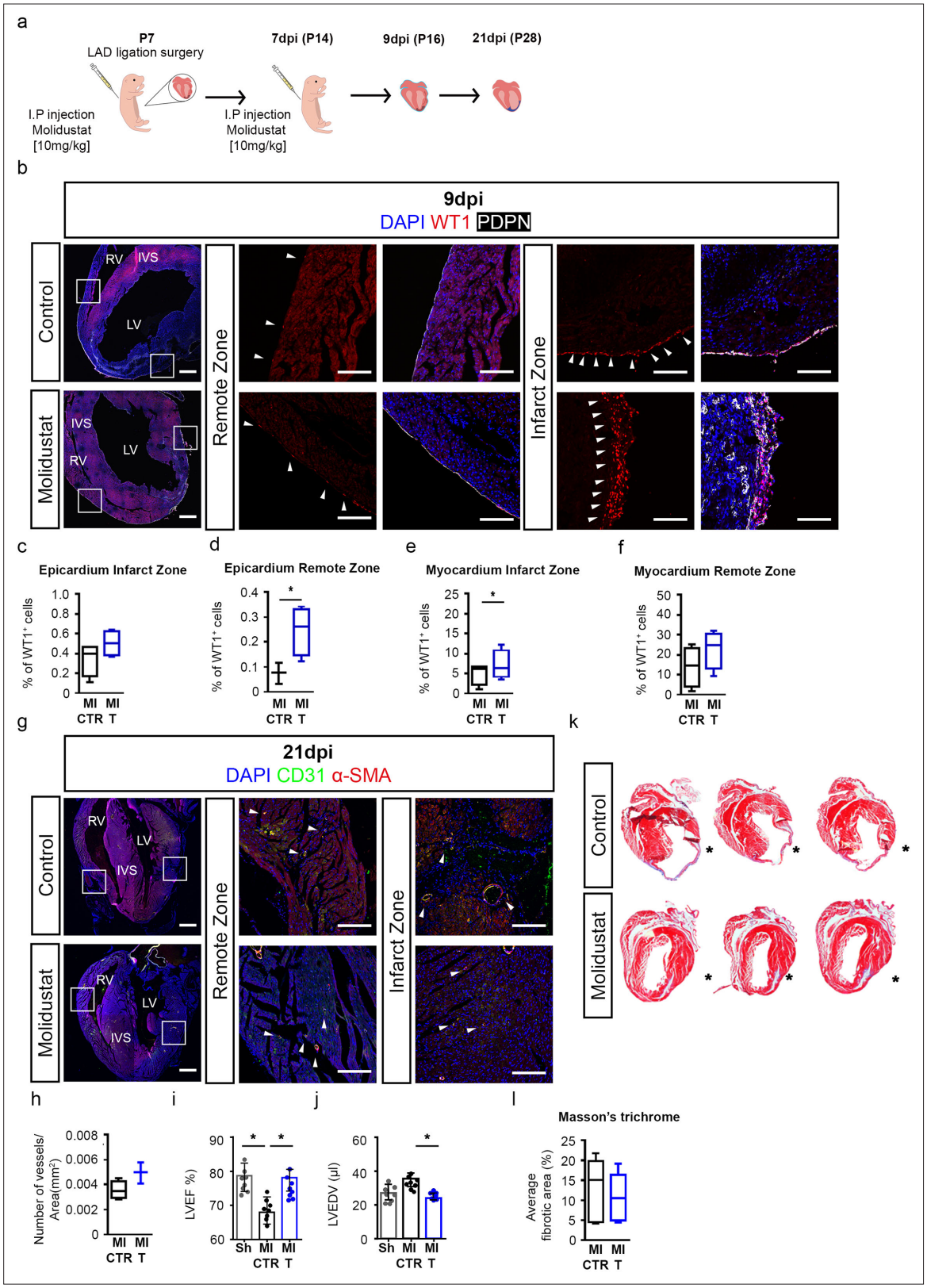

Figure 6. Pharmacological treatment with PHD inhibitors induces WT1 expression and improves heart function. (**a**) Schematic of experimental design. (**b**) Representative images of immunostaining for WT1 (red), PDPN (white), and DAPI nuclear stain (blue) on sections of hearts from animals treated with either saline (MI CTR) or Molidustat (MI T) and (**c–f**) quantification of number of WT1 positive cells at 9 days post-injury (dpi). Images on the right represent high magnification views of boxed regions shown in whole heart images. Arrowheads indicate expression of WT1 in the epicardium

Figure 6 continued on next page

Figure 6 continued

(determined by co-expression with PDPN). n=4 animals per group. (**g**) Representative images of immunostaining for CD31 (green), α-SMA (red), and DAPI (blue) on sections of hearts from animals treated with either saline (MI CTR, n=4) or Molidustat (MI T, n=4) and (**h**) quantification of number of vessels at 21dpi. Arrowheads indicate vessel (determined by co-expression of CD31 and α-SMA). Whole heart scale bars, 200 μm; high-magnification scale bars, 100 μm. Left ventricle (**i**) Ejection fraction (LVEF) and (**j**) end diastolic volume (LVEDV) evaluated by MRI analyses of non-infarcted (Sham, Sh; n=8), infarcted (MI CTR; n=8) controls and treated (MI T; n=8) hearts at 21dpi. (**k**) Representative images and (**l**) quantification of Masson's Trichrome stained transverse sections to assess cardiac fibrosis (blue) at 21 dpi. * denotes suture placement. Scale bars, 1 mm. IVS = interventricular septum, LV = left ventricle, RV = right ventricle. Scale bars 200 μm, high-magnification scale bars, 50 μm. Data presented as median, IQR and upper and lower limits and as mean ± s.e.m. *n* numbers refer to individual mice. Two-tailed, unpaired Student *t*-tests were used for statistical analysis between two groups, one-way ANOVA with Dunnett's post-hoc test was used for multiple comparisons in i and j. *p<0.05.

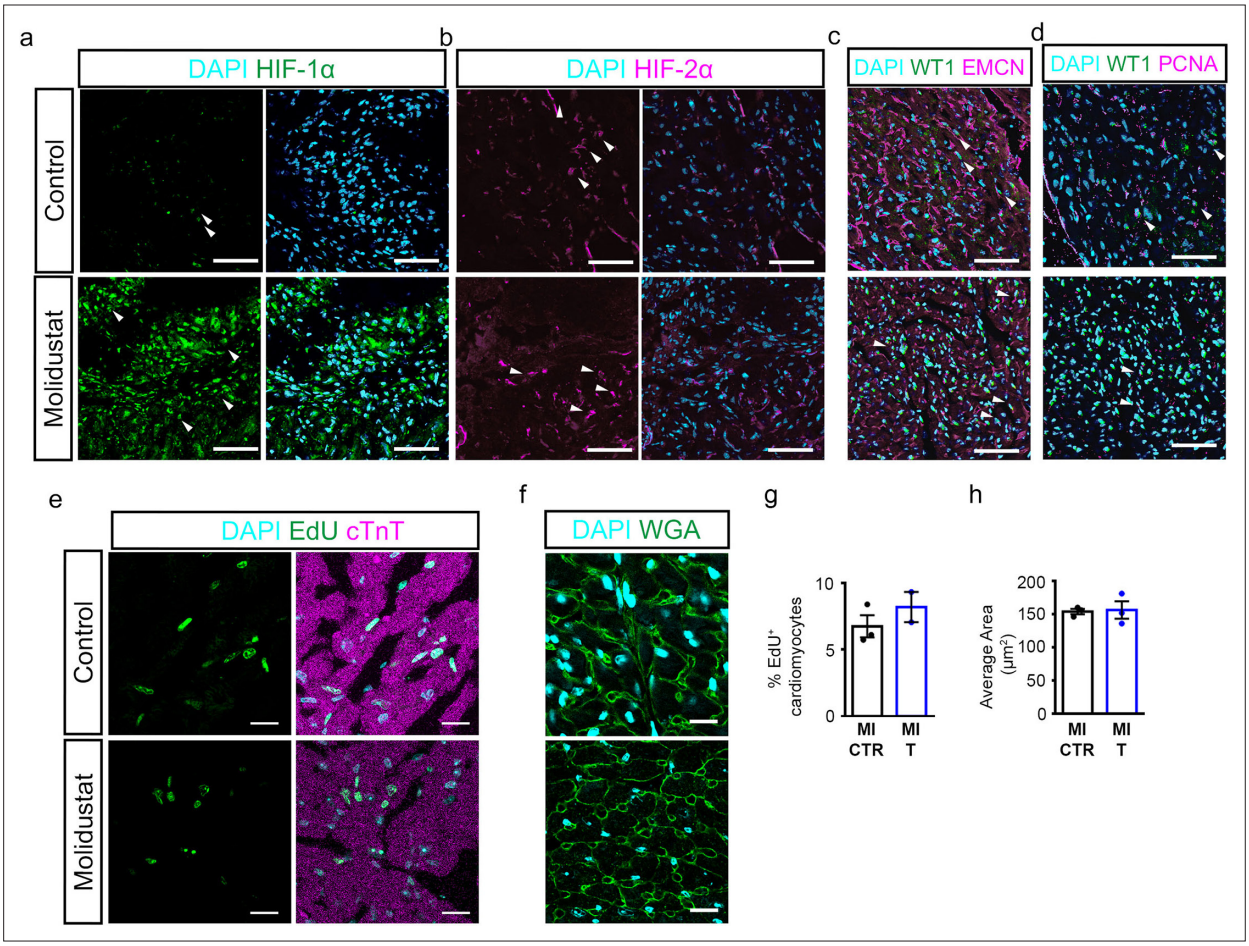

Figure 6—figure supplement 1. Effects of PHD inhibitor Molidustat administration to infarcted neonatal hearts at P7 and P14 on HIF signalling, cell proliferation, and hypertrophy. Representative images of immunostaining on cryosections of hearts from control and Molidustat treated mice 9dpi for: (**a**) HIF-1α (green), (**b**) HIF-2α (magenta), (**c**) WT1 (green) and EMCN (magenta), (**d**) WT1 (green) and PCNA (magenta), (**e**) EdU (green) and cardiac troponin T (cTnT, magenta), (**f**) wheat-germ agglutinin (WGA, green) and DAPI nuclear stain (cyan). Arrowheads indicate area of expression or co-expressing WT1/EMCN or WT1/PCNA. Scale bars, 100μm. (**g**) Quantification of EdU positive cardiomyocytes expressed as percentage of total cardiomyocytes in hearts from control (MI CTR, n=3) and Molidustat (MI T, n=2) treated mice. (**h**) Quantification of cardiomyocyte cell size, as assessed by WGA staining on sections of hearts from control (MI CTR, n=3) and Molidustat (MI T, n=3) treated mice. Left ventricular regions were measured. Error bars represent mean ± s.e.m. *n* numbers refer to individual mice. Two-tailed, unpaired Student t-tests were used for statistical analysis.